To Appear in *Astrophysical Journal*, Volume 565, 1 February 2002

An X-ray, Optical and Radio Search for Supernova Remnants in the Nearby Sculptor Group Sd Galaxy NGC 7793

Thomas G. Pannuti[1], Nebojsa Duric[2], Christina K. Lacey[3], Annette M.N. Ferguson[4], Marcus A. Magnor[5] and Caylin Mendelowitz[6]

ABSTRACT

This paper is the second in a series devoted to examining the multi-wavelength properties of supernova remnants (SNRs) located in nearby galaxies. We consider here the resident SNRs in the nearby Sculptor Group Sd galaxy NGC 7793. Using our own Very Large Array (VLA) radio observations at 6 and 20 cm, as well as archived *ROSAT* X-ray data, previously published optical results and our own Hα image, we have searched for X-ray and radio counterparts to previously-known optically-identified SNRs, and for new previously unidentified SNRs at these two wavelength regimes. Consistent with our prior results for NGC 300, only a tiny minority of the optically-identified SNRs have been found at another wavelength. The most noteworthy source in our study is N7793-S26, which is the only SNR in this galaxy that is detected at all three wavelengths (X-ray, optical and radio). It features a long ($\sim$ 450 parsecs) filamentary morphology that is clearly seen in both the optical and the radio images. N7793-S26's radio luminosity exceeds that of the Galactic SNR Cas A, and based on equipartition calculations we determine that an energy of at least 10^{52} ergs is required to maintain this source. Such a result argues for the source being created by multiple supernova explosions rather than by a single supernova event. A second optically-identified SNR, N7793-S11, has detectable radio emission but is not detected in the X-ray. A radio-selected sample of candidate SNRs has also been prepared by searching for coincidences between non-thermal radio sources and regions of Hα emission in this galaxy, and this search has

[1]MIT Center for Space Research, 77 Massachusetts Avenue, NE80-6015, Cambridge, MA 02139; tpannuti@space.mit.edu

[2]Institute for Astrophysics, Department of Physics and Astronomy, University of New Mexico, 800 Yale Blvd., N.E., Albuquerque, NM 87131

[3]Department of Physics and Astronomy, University of South Carolina, Columbia, SC 29208

[4]Kapetyn Astronomical Institute, University of Groningen, Postbus 800, Groningen 9700 AV, The Netherlands

[5]Computer Graphics Laboratory, Department of Computer Science, Stanford University, Gates Building, Room 360, Stanford, CA 94305-9025

[6]Science Department, The Evergreen State College, 2700 Evergreen Parkway NW, Olympia, WA 98505

yielded five new candidate radio SNRs, to be added to the 28 SNRs that have already been detected by optical methods. A complementary search for new candidate X-ray SNRs has also been conducted by searching for soft-spectrum sources ($kT < 1$ keV) that are coincident with regions of Hα emission. That search has yielded a candidate X-ray SNR which is coincident with one (and possibly two) of the candidate radio SNRs, but considerable diffuse X-ray emission throughout the disk of NGC 7793 reduces the efficacy of the search. Like NGC 300, very little overlap in identifications is seen between the SNRs found through X-ray, optical and radio methods, and such a result argues for the role played by distance-dependent selection effects in determining the detectability of SNRs. In addition, we find that the density of the ambient interstellar medium (ISM) surrounding SNRs significantly impacts the spectral characteristics of the SNRs in this galaxy, consistent with surveys of the SNR populations in other galaxies.

Subject headings: galaxies: individual (NGC 7793) — galaxies: ISM — galaxies: spiral — radio continuum: galaxies — X-rays: galaxies — supernova remnants

1. Introduction

This paper is the second in a series devoted to the multi-wavelength study of supernova remnants (SNRs) in nearby galaxies. In our previous paper (Pannuti et al. 2000, hereafter referred to as Paper I) we analyzed observations made at the X-ray, optical and radio wavelengths of the nearby Sculptor Group Sd galaxy NGC 300. We sought to determine the X-ray and radio properties of the 28 SNRs identified previously in that galaxy through optical search techniques, namely Hα and [S II] narrow-band imaging (D'Odorico et al. 1980; Blair & Long 1997, hereafter referred to as BL97), and in addition, we searched for new candidate SNRs at the X-ray and radio wavelengths to complement this prior optical work. Our search yielded sixteen new candidate X-ray and radio SNRs, later reduced to fifteen by the recent work of Read & Pietsch (2001), and the total number of SNRs and candidate SNRs in NGC 300 is now 43. We found very little overlap between the three sets of selected candidates, and we interpret this to indicate that a multiple-wavelength approach is necessary to detect a maximum number of candidate SNRs in a particular galaxy. We also hypothesized that the limited overlap between the selected sets of candidate SNRs indicated selection effects inherent in each type of survey: optical surveys are biased toward the detection of SNRs located in regions of low density and corresponding low optical confusion, while X-ray and radio surveys have the opposite bias and favor the detection of SNRs located in regions of high density.

In this paper, we examine another Sculptor Group Sd galaxy, NGC 7793, and once again we consider observations made at the X-ray, optical and radio wavelengths. Following the paradigm set by our previous work (Paper I), our intent is to determine the X-ray and radio properties of the previously-known optically-identified SNRs as well as search for new candidate SNRs at those

two wavelengths. Salient properties of NGC 7793 are listed in Table 1: Puche & Carignan (1988) measured a distance to this galaxy of 3.38 Mpc and classified it as a member of the Sculptor Group of galaxies. Because of its proximity and its low inclination angle of 50° (Tully 1988), this galaxy makes an excellent choice for the study of galactic properties. These studies include an optical survey for resident SNRs (BL97), analyses of its HI content (Carignan & Puche 1990), its surface photometry (Carignan 1985) and its radio continuum properties (Harnett 1986). Its X-ray properties have also been the subject of X-ray analysis, based on observations performed with the *Einstein* satellite (Fabbiano et al. 1992) and later observations performed with the *ROSAT* satellite (Read & Pietsch 1999, hereafter referred to as RP99). In Section 2, we describe the observations of this galaxy and data reduction at each wavelength, beginning with the radio (Section 2.1), followed by the optical (Section 2.2) and concluding with the X-ray (Section 2.3). We discuss the multi-wavelength properties of the optically-selected SNRs in Section 3, and then present the new candidate SNRs selected at the radio and X-ray wavelengths in Sections 4 and 5. A discussion of our findings in this work is presented in Section 6 and finally our conclusions are given in Section 7.

2. Observations and Data Reduction

2.1. Radio Observations and Data Reduction

We observed NGC 7793 with the Very Large Array (VLA) of the National Radio Astronomy Observatory (NRAO[7]) at a wavelength of 6 cm (4885 MHz) in the hybrid CnB configuration (northern arm in B array) on 1993 May 22 and at a wavelength of 20 cm (1465 MHz) in the hybrid BnA configuration (northern arm in A array) on 1998 June 13. The greater north-south coverage provided by the extended northern arms in these two arrays make them well-suited for studying such southern galaxies as NGC 300 (Paper I) and NGC 7793 (the present paper). The approximate beam sizes in the final images are $\approx 6''$ at 6 cm (4885 MHz) and $\approx 6''$ at 20 cm (1465 MHz), and the RMS noise measured in each image is 32 μJy/beam and 60 μJy/beam at 6 cm and 20 cm, respectively. Details of the VLA observations are provided in Table 2.

Our strategy for observing this galaxy was similar to the one described in Paper I for observing NGC 300. Once again, to minimize bandwidth smearing effects that may limit the field of view when observing in normal continuum mode, we observed NGC 7793 in multichannel line mode with eight channels per intermediate frequency (IF), including the continuum calibrating channel (the zeroth channel), and a channel width of 3.125 MHz. Of the seven spectral channels, the seventh was discarded because its response decreased markedly, and the bandpass correction needed to address this low response was both rather high and a possible source of error. A total band of 37.5 MHz

[7]The National Radio Astronomy Observatory (NRAO) is a facility of the National Science Foundation operated under cooperative agreement by Associated Universities, Inc.

was synthesized after the seventh channel was dropped. The effective observing frequencies for the images made from the remaining six channels were 1.448 GHz and 4.860 GHz at 20 cm and 6 cm, respectively. Data reduction and analysis were performed using the AIPS software package, which is a standard data reduction package provided by the NRAO. The final images were corrected for primary beam attenuation before undertaking flux measurements.

For the analysis of the radio sources in this galaxy, we repeated the procedure described previously in Paper I: again, our primary goal was to find and measure all discrete sources above a minimum 3 σ detection level at both 6 and 20 cm. Peak positions of the identified sources were determined by fitting single Gaussians to their emission profiles at 20 cm. Routines in AIPS were used to identify the flux density associated with each source: by using annuli that were approximately $1''$ in width, we determined the flux density based on the cumulative flux density minus the average flux density at an outer annulus chosen to represent the background level.

The spectral index α of each source (defined by the convention $S_\nu \propto \nu^{-\alpha}$) was calculated from the measured 6 cm and 20 cm flux densities, denoted as S_6 and S_{20}, respectively. The uncertainties in each spectral index were determined by propagation of errors. Those radio sources that were coincident with regions of Hα emission in NGC 7793 and featured non-thermal spectral indices formed the set of radio sources from which the sample of candidate radio SNRs was assembled (as described in Section 4). For our selection criterion, we classified those radio sources with spectral indices $\alpha \geq 0.2$ as candidate radio SNRs. This criterion is consistent with the previous searches for candidate radio SNRs in the galaxies NGC 300 (Paper I) and NGC 6946 (Lacey et al. 1997). Properties of these sources (positions in J2000.0 coordinates, flux densities at 6 and 20 cm and spectral index α) are listed in Table 3.

2.2. Optical Observations and Data Reduction

NGC 7793 was observed and imaged using an Hα filter by the 1.5 meter telescope at the Cerro Tololo InterAmerican Observatory (CTIO)[8] on the nights of 1993 December 14-18 and 1994 September 28-October 2. The observational data and its analysis are presented in Ferguson et al. (1996), and the reader is referred to that work for more information.

NGC 7793 was observed as part of a study of the diffuse ionized gas (DIG) found in this galaxy as well as another Sculptor Group galaxy, NGC 247. The DIG was found to account for between 30% and 50% of the diffuse Hα emission in this galaxy, compared to between 44% and 54% for NGC 300 as found by Hoopes et al. (1996). Greenawalt et al. (1998) have found that the DIG accounts for between 40% and 50% of the Hα emission from three other galaxies – namely M51, NGC 5195 and M81 – and it appears that generally speaking, the DIG accounts for approximately this fraction of

[8]The CTIO is operated by AURA, Inc., under cooperative agreement with the National Science Foundation as part of the National Optical Astronomy Observatories.

Hα emission within spiral galaxies. The presence of considerable DIG in NGC 7793 (especially when the DIG accounts for such a high fraction of a galaxy's diffuse Hα emission) suggests that extensive star formation is taking place in this galaxy. This current epoch of widespread star formation will certainly produce a population of SNRs that will be detectable by our multi-wavelength survey.

The 28 SNRs found in NGC 7793 by BL97 were detected through narrow-band imaging of this galaxy using Hα and [S II] filters. A particular source was identified as an SNR candidate if the ratio of its fluxes [S II]/Hα exceeded 0.4. We will examine the X-ray and radio properties of these sources in Section 3. For the present work, we will also make use of the catalog of HII regions in this galaxy that was prepared by Hodge (1969), based on observations made using the Palomar 48-inch telescope. In that paper, NGC 7793 was one of twenty galaxies that had its HII region population surveyed and cataloged for future reference purposes. As a result of that survey, 35 HII regions were identified in this galaxy, and we will use this list to identify HII regions that may be associated with SNRs. We note that the survey presented in that paper was biased toward the detection of only the brightest HII regions in NGC 7793, and for that reason numerous faint HII regions were not listed.

2.3. X-ray Observations and Data Reduction

We used archived observations of NGC 7793 made with the wide-angle, spectral-resolving Position Sensitive Proportional Counter (*PSPC*) instrument aboard the *ROSAT* satellite (Trümper 1992). NGC 7793 was observed over two separate epochs with the *PSPC* instrument: the first epoch was on 1992 December 7 for 13332 seconds and the second was between 1993 May 20 and 1993 May 27 for 10507 seconds. Data from these two observing epochs were combined to produce images corresponding to a total integration time of 23839 seconds. Following the example set by Long et al. (1996) in their study of the X-ray sources in M33 and similar to our previous analysis of X-ray emission from NGC 300 (Paper I), images were prepared at the three energy bands defined as the "total" (0.1-2.4 keV), the "hard" (1.0-2.4 keV) and the "soft" (0.1-1.0 keV) from combining data for the two separate observation epochs.

This *PSPC* data of NGC 7793 has already been discussed in detail by RP99, and in their analysis 27 sources were identified at a 4σ detection level or higher in the central $25' \times 25'$ area of the field of view. Of these 27 sources, seven (denoted as P6, P7, P8, P9, P10, P11 and P13 in their notation) fell within the optical extent of the galaxy. We will concentrate on these particular seven X-ray sources to avoid confusion with X-ray emission from background sources (such as distant AGN's and quasars), and we present properties of these sources (source numbers, positions, net numbers of counts at the total band, fluxes, hardness ratios and probabilities of variability), as measured by those authors, in Table 4. These fluxes given by RP99 were determined by assuming a 5 keV thermal bremsstrahlung and a hydrogen column density of $N_H = 1.14 \times 10^{20}$ cm^{-2}. The hardness ratios correspond to the particular ratio denoted as "HR1" by RP99, which is the ratio defined as (hard counts - soft counts)/(hard counts + soft counts). In the last column, we list optical

and radio counterparts to each X-ray source, drawing from the sample of radio sources described in Section 2.1, the optically-identified SNRs found by BL97 and the catalog of HII regions found by Hodge (1969). The HII regions are referred to by their catalog number; *e.g.*, #31 in that catalog is listed as H31. In Figure 1, the X-ray emission in the "total" band from NGC 7793 (as observed by the *ROSAT PSPC*) is depicted in contours, with Hα emission shown in gray-scale.

The population of X-ray sources within the disk of NGC 7793 is expected to be a mixture of X-ray binaries and SNRs, and a spectral analysis can help differentiate between these two classes of sources. Schulz (1999) has found that the spectra of X-ray binaries with low foreground column densities (which is applicable for the present study of sources in NGC 7793) can be best fit with power laws, while in contrast the X-ray spectra of SNRs is best fit using thermal bremsstrahlung models (Hwang et al. 2000). Effects of thermal continuum absorption at radio wavelengths along Galactic lines of sight are discussed by Lacey et al. (2001): those authors discovered such absorption toward the Galactic SNR W49B by an intervening complex of HII regions and analyzed how this absorption affects the observed radio spectrum of the SNR. Searching for variations in the luminosities of the X-ray sources detected in NGC 7793 gives an additional method for classifying these sources as either X-ray binaries or SNRs: X-ray binaries can exhibit a time dependence to their luminosities (as will other classes of variable X-ray sources), while the X-ray emission from SNRs should be nominally time-independent. By considering these differences in X-ray emission characteristics between SNRs and X-ray binaries, we should be able to generally differentiate between sources of these two types. We hasten to add, however, that these distinctions cannot be viewed as absolute ways to classify these sources. For example, Schulz (1999) points out that a combination of a power law model and a thermal bremsstrahlung model is required to optimize fits to the spectra of X-ray binaries, and likewise some SNRs are known to possess components to their X-ray emission which have a power law dependence (Allen et al. 1997). Finally, if the period of the X-ray binary's emission exceeds the integration time for an X-ray observation of a galaxy, it may appear to be constant in X-ray luminosity and lead to an incorrect classification. Nonetheless, we will still make use of these general differences in the properties of X-ray emission from SNRs and X-ray binaries in order to approximately classify these sources, and we note that more rigorous classifications must await X-ray observations of this galaxy with superior quality.

We point out that at a distance of 3.38 Mpc (Puche & Carignan 1988), NGC 7793 is considerably more distant than NGC 300, which is located at a distance of 2.1 Mpc (Freedman et al. 1992) and was the subject of our previous study (Paper I). For this reason, while our angular resolution is the same in both of these studies, our spatial resolution of structures in NGC 7793 is reduced. In addition, while only a modest amount of diffuse X-ray emission was found in NGC 300 by Read & Pietsch (2001), such emission was clearly detected in the disk of NGC 7793 by RP99, with a characteristic energy kT of approximately 1 keV. This diffuse emission makes it difficult to clearly associate X-ray emission with point sources found at other wavelengths in this galaxy. We will return to this point in the remaining sections of this paper.

3. Multi-Wavelength Properties of the Optically-Selected SNRs in NGC 7793

In our prior study of the optically-identified SNRs in NGC 300, we found that most of the SNRs selected in this manner were weak or undetected in the X-ray and radio (Paper I). We hypothesized that such a result may indicate a selection effect inherent in optical surveys, which are more sensitive to detecting SNRs in regions of lower density in a galaxy. Such SNRs may be weak emitters in the X-ray and radio because of their location within diffuse environments, which are not conducive to high X-ray and radio luminosities. In contrast, SNRs which are powerful sources of X-ray and radio emission are often located in regions of high density (such as HII regions), and precisely because of their location they may be missed by optical surveys, which are subject to considerable confusion from diffuse emission in these regions. It is generally believed that SNRs which are located in regions of low density were parented by low-mass white dwarf progenitor stars as Type Ia supernovae (SNe), while in contrast SNRs which are found in regions of high density (such as spiral arms) were created by high-mass progenitor stars as Type II SNe (Bartunov et al. 1994). However, exceptions have been pointed out for both of these assertions: as examples, we note that an isolated high-mass star may produce a Type II SNe in a region of comparatively low density, and a Type Ia SNe may occur in a spiral arm of a galaxy (a location of enhanced density) given the long lifetimes of white dwarf stars.

For our samples of extragalactic SNRs, however, information about the type of SN that produced each SNR is usually not available. Therefore, our studies of SNRs in other galaxies encompass SNRs produced by both low-mass and high-mass progenitor stars and therefore sample much of the galaxy's star formation history. We argue that by conducting surveys for SNRs in the X-ray, optical and radio, we can probe regions of galaxies over a wide range of densities and thus detect a maximum number of SNRs in galaxies, including SNRs that have been produced by both types of SNe and progenitor stars.

In our study of the optically-identified SNRs in NGC 7793, we discovered errors in the published positions of these SNRs as given by BL97. We found that while the published right ascension positions for the SNRs located in the eastern half of the galaxy appeared to be reasonably accurate – that is, within the quoted positional errors of $\approx 2''$ (BL97) – the accuracy of the listed right ascension positions declined markedly for the SNRs in the galaxy's western half. In particular, the accuracy in the published right ascension of the SNRs was considerably beyond the quoted positional errors for the SNRs N7793-S1 through N7793-S12. For N7793-S12, we found a difference of approximately $19''$, and this difference increased gradually as we considered SNRs in turn located toward the galaxy's western edge, culminating with $37''$ for N7793-S1. We note that the published declination positions were accurate within the quoted positional errors for the entire sample of optically-identified SNRs. To determine the correct right ascension coordinates of the optically-identified SNRs, we measured the positions of the SNRs as seen in our Hα image based on the images of these sources as presented by BL97, and we give the corrected positions in Table 5. After confirming that we had located the SNRs identified by BL97, we proceeded to analyze their X-ray and radio properties.

Of the 28 SNRs found in NGC 7793 by BL97 using optical methods, only two were detected at another wavelength at the 3 σ level or higher. N7793-S11 was detected as a non-thermal radio source with flux densities of 0.27±0.06 mJy and 0.42±0.12 mJy at the wavelengths of 6 and 20 cm, respectively, corresponding to a spectral index α of 0.4±0.2. No X-ray counterpart was detected for this source, though a search for a counterpart is complicated by the diffuse X-ray emission within the disk of this galaxy. We did find both X-ray and radio counterparts to the source N7793-S26, an SNR which also has a filamentary extension denoted as N7793-S26ext by BL97. For the remainder of this paper, we will refer to both the source N7793-S26 and its filamentary extension N7793-S26ext as N7793-S26. We present a listing of the spectral properties of these two optically-identified SNRs in Table 3, and multi-wavelength images of these two optically-identified SNRs are presented in Figures 2 and 3 respectively.

N7793-S26 is a particularly interesting source, and we will devote some discussion to its properties here. It is readily apparent in optical images that the source's morphology is that of a long filament, and this morphology is imitated remarkably in the radio, as seen by inspection of the images presented in Figure 3. RP99 first identified the X-ray counterpart to N7793-S26 source (labelled by those authors as P8) and attempted to fit its X-ray spectrum using two models (namely a thermal bremsstrahlung model and a blackbody model). While the goodness of the model fits (χ^2's of 0.21 and 0.16, respectively) do not strongly favor one model over the other, we do note that the fit parameter for the blackbody model returned an energy value of $kT = 0.17\pm0.05$ keV, while the corresponding energy value for the thermal bremsstrahlung model is $kT = 0.36\pm0.25$ keV. Both of these energy values are consistent with that expected for the X-ray emission from an SNR. In addition, RP99 also performed a test to search for variability in the emission from the X-ray sources in NGC 7793, and found that the probability of variability in P8's X-ray emission was only 13%, also consistent with the type of X-ray emission expected from SNRs. We will discuss the variability of X-ray emission from the X-ray sources in NGC 7793 more extensively in Section 5.

As part of their analysis, RP99 examined an NRAO VLA Sky Survey (NVSS) 1.4 GHz radio continuum image of NGC 7793, and found a radio counterpart to N7793-S26 to complement the X-ray and optical detections. This three-wavelength detection enhances the likelihood that this source is either a collection of several SNRs or a single large and luminous SNR. No quantification of the radio emission properties (such as flux densities) was given by RP99 for this source, but by examining our 6 and 20 cm images we measure flux densities for the entire structure of 1.24±0.19 mJy and 3.75±0.30 mJy at 6 and 20 cm, respectively, with a corresponding spectral index of α=0.9±0.2. At the assumed distance of 3.38 Mpc for NGC 7793, the most radio-luminous Galactic SNR, Cas A, would have a flux density of 2.8 mJy at 20 cm, which is about 75% of the observed flux density for N7793-S26 at that same wavelength. Clearly, this is an extremely luminous radio source, and its filament-like morphology with a length of approximately 450 parsecs makes this source even more intriguing.

The unusual properties of this source have led to speculation about its true nature. It is

possible that this source was produced by the collective expansion of several SNRs that were created at approximately the same time, therefore indicating that N7793-S26 may be a nascent superbubble structure. Matonick et al. (1997) argue that the maximum attainable size of an SNR expanding into an interstellar medium (ISM) with a mean number particle density of between 0.1 and 1 cm^{-3} (a typical Galactic value) is approximately 100 parsecs. In addition, based on equipartition calculations where we assume a radius of 225 pc for N7793-S26, consistent with its apparent size, we determine that an energy of at least 10^{52} ergs is required to maintain this source (Pannuti et al. 2002, in preparation), far greater than the energy yield expected from a single SN. All of this evidence suggests that N7793-S26 was not produced by a single supernova explosion of average energy.

BL97 investigated the nature of N7793-S26 by searching for an interior star cluster within the SNR. The presence of such a cluster would argue in favor of the collective supernova remnant hypothesis. Those authors found no evidence for such an interior star cluster, but their data lacked the precision required to answer this question decisively. Therefore, the true nature of this object has yet to be determined, and it will likely be the subject of further study at multiple wavelengths.

To summarize the results of this section, of the 28 optically-identified SNRs detected in this galaxy by BL97, only two possess counterparts at another wavelength: N7793-S11 in the radio and N7793-S26 in both the X-ray and the radio. Consistent with our previous findings for the SNR population in NGC 300 (Paper I), no X-ray or radio emission has been found from the large majority of the optically-identified SNRs in NGC 7793. The results of our complementary searches for candidate radio and X-ray SNRs are presented in Sections 4 and 5, respectively.

4. Properties of the Radio-Selected SNR Candidates

Our radio observations of NGC 7793 have yielded five candidate radio SNRs, to be added to the 28 SNRs previously known through the optical survey conducted by BL97. We present images that depict the multi-wavelength properties of these candidate radio SNRs in Figures 4 through 8, using a similar format to that used for the images of the optically-identified SNRs as shown in Figures 2 and 3. Similar to our search for candidate radio SNRs in NGC 300 (Paper I), these sources have been chosen based on their non-thermal radio emission and their association with regions of Hα emission in NGC 7793. Extensive optical confusion in these regions may have prevented the prior detection of these sources by optical methods. We find that the radio emission from some of these candidate radio SNRs is confused with diffuse thermal emission from the region of Hα emission itself. This affects two of our five candidate radio SNRs – namely NGC 7793-R3 and NGC 7793-R4 – and is similar to the situation we encountered in our previous study of candidate radio SNRs in NGC 300. Because of the larger distance to NGC 7793 compared to NGC 300, our survey for candidate radio SNRs has a corresponding reduction in sensitivity, and only the more luminous candidate radio SNRs in this galaxy are detected by our survey.

Following the paradigm set in our analysis of candidate radio SNRs in NGC 300 (Paper I), we have sought coincidences between our sample of radio sources and the list of X-ray sources identified in this galaxy by RP99. We have found one such coincidence: the candidate radio SNR NGC 7793-R3 is coincident with the X-ray source P10 as identified by RP99, with an offset of only $\sim 5''$. This offset is well within the typically-quoted spatial resolution of the *PSPC* instrument, namely a 90% enclosed energy radius at 1 keV of $27''$ (Hasinger et al. 1992). Both the X-ray source and the radio source correspond to the HII region Hodge 23, as cataloged by Hodge (1969). RP99 used two thermal bremsstrahlung models to fit the spectra of this source, and both of the resultant fits correspond to spectral energy distributions that peak below 1 keV (0.77±0.64 and 0.63±0.52 keV, respectively), consistent with the X-ray spectra expected for an SNR. The luminosity estimates for this source are approximately 10^{38} ergs sec^{-1} at the assumed distance to NGC 7793, which is rather large for a single individual SNR. It is very likely that this fit incorporates diffuse emission in the neighborhood of the SNR that was not resolved by the *ROSAT PSPC* observations, or it may be that additional X-ray flux is supplied by other SNRs in the region. We note that a second candidate radio SNR was found in an adjacent region of Hα emission (NGC 7793-R4 in the HII region Hodge 21), but the offset of this second source is considerable ($\sim 15''$). Higher resolution X-ray observations of this source may lead to a clearer interpretation of its properties.

To complete this discussion on radio-selected SNRs, we consider background radio sources seen through the disk of NGC 7793 and the potential confusing effects such sources may have on this survey. We repeat two tests to study the possible effects of background source confusion that we first presented in our previous study of NGC 300 (Paper I). First, we use the estimates of Mitchell & Condon (1985) for the number density of background radio sources at 20 cm and determine that approximately four background sources at that wavelength should be detected in random directions through the disk of NGC 7793 at a 3 σ level of 0.2 mJy or greater. Similarly, a search for position coincidences between "negative" radio sources that are detected at the -3 σ level with regions of Hα emission yielded only one such coincidence, which is consistent with the result expected from random superpositions of these background sources with regions of Hα emission seen in NGC 7793. As we noted with NGC 300, while the criteria for our radio survey for SNRs selects against isolated radio-emitting SNRs, we do detect SNRs located within dense regions of Hα emission, and therefore we can estimate the number of SNRs missed by optical surveys.

5. Properties of the X-ray-Selected SNR Candidates

In order to complete our multi-wavelength search for SNRs in NGC 7793, we will now discuss the X-ray sources previously described in Section 2.3. The X-ray source P8 and its association with the optically-identified SNR N7793-S26 has already been discussed in Section 3. Likewise, the association between the X-ray source P10 and the candidate radio SNR NGC 7793-R3 has already been presented in Section 4. We will now consider the five remaining X-ray sources found within the disk of NGC 7793 by RP99 to determine if any of these remaining sources may be candidate X-ray

SNRs. We note that it is possible that an X-ray source seen through the disk of NGC 7793 may actually be a background source unrelated to the foreground galaxy. To address this possible source of confusion, we will only consider those X-ray sources which also possess an optical counterpart within the galaxy to be candidate X-ray SNRs.

As was the case in our study of X-ray sources in NGC 300 (Paper I), we will consider an X-ray source to be a candidate X-ray SNR if it satisfies two criteria: first, the X-ray source must not show convincing evidence for time variability in its X-ray luminosity, and second, it must possess a spectrum which can be optimally fit using a thermal bremsstrahlung model with a characteristic temperature kT of 1 keV or less. To apply the first criterion, we note that while analyzing their X-ray data for this galaxy, RP99 measured the count rates over the two observing epochs for each of the 27 sources detected within the field of the *ROSAT PSPC* observations of NGC 7793. Based on these count rates, RP99 also determined the probability of variability for each source. We reproduce the results of their analysis in Table 4, and note that for the two X-ray sources P9 and P13, RP99 determined a 100% probability of variability. On the basis of that finding, we discard those two sources from consideration as candidate X-ray SNRs. The two X-ray sources which we have already associated with SNRs (P8 and P10) both show only slight evidence for X-ray variability (probabilites of 13% and 7%, respectively). As for the second criterion, we note that the X-ray source P11 was best-fit by RP99 using a power-law model rather than a thermal bremsstrahlung model, and for that reason P11 was not considered a candidate X-ray SNR.

The above analysis leaves two X-ray sources to consider, P6 and P7. Unfortunately, it is not a straightforward matter to determine the true nature of either of these sources. In our previous analysis of X-ray sources in NGC 300 (Paper I), we could isolate the candidate X-ray SNRs on the basis of spectra which, according to the fits produced by Read et al. (1997), appeared to favor one spectral-fitting model (power law or thermal bremsstrahlung) over the other. Inspection of the computed χ^2's for each model (calculated to evaluate the quality of each fit) shows that neither of the two models is distinctly superior to the other for either of the two sources. Such ambiguity originates from the low count rates registered by each source ($1.8\pm0.4 \times 10^{-3}$ and $2.4\pm0.5 \times 10^{-3}$ counts sec^{-1} for P6 and P7, respectively), and it prevents the conclusive classification of each source. RP99 argue that these sources may be background objects unrelated to NGC 7793, on the basis of the similarity of their spectra with quasars, the lack of optical counterparts in NGC 7793 for both of these sources, and their possible associations with faint stellar-like objects, with apparent magnitudes m_V of 16 and 18, respectively. The somewhat high likelihood of variability for these sources (41% and 37%, respectively) are also arguments against classifying these sources as candidate X-ray SNRs. Inspection of our own radio images fails to reveal sources at either the 6 or 20 cm wavelengths at the 3σ level or higher that are associated with P6 or P7. A true understanding of these sources must therefore await additional observations, and we therefore do not consider either of these sources to be new candidate X-ray SNRs. To summarize the results of this section, we have not found any new candidate X-ray SNRs besides the previously discussed X-ray sources P8 and P10.

6. Discussion

As a result of our X-ray and radio searches for SNRs in NGC 7793, five new SNRs have been detected, to be added to the list of 28 optically-identified SNRs found in this galaxy by BL97. All five of these SNRs are candidate radio SNRs, and one of them – NGC 7793-R3 – possesses a counterpart in the X-ray. Another candidate radio SNR, NGC 7793-R4, may also be associated with this X-ray source. In Table 6, we present a listing of cross-references for these new SNRs. The surprising lack of overlap in detected SNRs found by the three different search techniques – X-ray, optical and radio – is consistent with our results for NGC 300 (Paper I). A similar result has been found by Lacey & Duric (2001) in the case of the nearby galaxy NGC 6946: those authors found very limited overlap between the sample of candidate radio SNRs presented by Lacey et al. (1997) and the sample of optically-identified SNRs prsented by Matonick & Fesen (1997) in that galaxy. In Figure 9, we present Venn diagrams to depict the amount of intersection seen between selected sets of SNRs in the galaxies NGC 300, NGC 7793 and M33: we have prepared these diagrams for NGC 300 and NGC 7793 based on the results of Paper I and the present work, respectively, while the diagram for M33 has been created based on results from Haberl & Pietsch (2001), Gordon et al. (1998) and Gordon et al. (1999). We note that we have updated the Venn diagrams for both M33 and NGC 300 from Paper I in light of recent work on the X-ray source populations in those two galaxies as presented by Haberl & Pietsch (2001) and Read & Pietsch (2001), respectively. Here we briefly describe the impact of these two recent works on the Venn diagrams: a detailed study of the SNR population in NGC 6946, based on X-ray, optical and radio observations, as well as a statistical study of the properties of candidate radio SNRs in nearby galaxies, will be the subjects of future papers.

In their study of the X-ray population of M33, Haberl & Pietsch (2001) prepared a catalog of X-ray sources in that galaxy based on data from *ROSAT PSPC* and *HRI* (High Resolution Imager) observations. A total of 184 sources were detected within 50 arcminutes of the nucleus, an increase in the number of known X-ray sources in this galaxy as detected by Long et al. (1996) by over a factor of three. Haberl & Pietsch (2001) classified sixteen of the 184 sources as SNRs based on their spectral properties, of which eleven are also detected in the optical and radio, two are also detected in the optical but not the radio, and the remaning three are not found at either of the other two wavelengths. Haberl & Pietsch (2001) noted that only thirteen of the 98 SNRs found by Gordon et al. (1998) using optical methods are also detected in the X-ray, and suggested that the optically-identified SNRs that lack X-ray emission are likely expanding into a low density ISM.

Similar to the work presented by Haberl & Pietsch (2001), Read & Pietsch (2001) examined *ROSAT PSPC* and *HRI* observations of NGC 300 and, through their analysis, increased the number of *PSPC* detected sources within the disk of NGC 300 from the fifteen presented by Read et al. (1997) to 26. Read & Pietsch (2001) refuted the classification by Paper I of two X-ray sources as candidate X-ray SNRs, namely the sources denoted as P44 and P56 by Read & Pietsch (2001). P44 was re-classified by those authors as an X-ray binary (thereby calling into doubt its association with the candidate radio SNR R2 as claimed by Paper I) while P56 was classified as a foreground star.

Read & Pietsch (2001) identified six candidate X-ray SNRs, three of which (P29, P38 and P49, in their notation) are associated with three optically-identified SNRs cataloged by BL97 (N300-S6, N300-S10 and NGC 300-26, respectively). Using these new results and retaining the association (as argued in Paper I) between the X-ray source denoted as P41 by Read & Pietsch (2001) and the candidate radio SNR R5, we have revised the Venn diagram for NGC 300 accordingly.

Considering these three Venn diagrams and returning to the argument we presented in Paper I, we feel that the driving effect for such limited intersection is the distance to the galaxy. The sensitivities at all three wavelengths for the surveys in all three galaxies are presented in Table 7: we note that we have updated the sensitivities of the X-ray surveys in M33 and NGC 300 from Paper I in light of the recent work presented by Haberl & Pietsch (2001) and Read & Pietsch (2001), respectively. Because the sensitivities of the surveys for each galaxy are very similar for each wavelength, we argue that distance plays the most dramatic role in determining the likelihood of detecting an SNR.

Furthermore, our results for NGC 7793 represent the third example of a galaxy (following NGC 300 and NGC 6946) where very few of the SNRs found by optical methods are also seen in the X-ray and radio. We interpret this result to suggest that optical surveys favor the detection of SNRs located in regions of lower density, and may therefore select the SNRs produced by Type Ia SNe. In contrast, radio and X-ray surveys for SNRs in a galaxy are biased toward the detection of SNRs located in regions of high density, and therefore may preferentially select the SNRs that were most likely produced by Type II SNe. Therefore, the density of the ambient ISM surrounding an SNR is strongly linked to the spectral characteristics of the SNR. Additional observations and analysis are needed to more thoroughly explore these results.

7. Conclusions

We have presented a multi-wavelength search and analysis of the SNR population in NGC 7793. The results and conclusions of this work can be summarized as follows:

1) NGC 7793, a nearby spiral galaxy, has been observed in the X-ray, optical and radio wavelengths to analyze its resident SNR population. This analysis has examined X-ray observations of the galaxy made by the *ROSAT PSPC* instrument, an Hα image of the galaxy and new 6 and 20 cm observations made with the VLA. We have analyzed both the X-ray and radio spectral properties of the SNRs previously identified in the optical by BL97, and in addition we have searched for new candidate X-ray and radio SNRs.

2) N7793-S26 is the only optically-identified SNR that possesses both X-ray and non-thermal radio emission. The extreme radio luminosity of this object and its large filamentary structure have led to speculation about its creation. A study of the energetics of this SNR suggest that it was created by multiple supernova explosions rather than a single supernova event. One other optically-identified SNR, N7793-S11, possesses non-thermal radio emission but no X-ray emission.

Consistent with prior studies of the SNR populations in the galaxies NGC 300 and NGC 6946, X-ray and radio emission from optically-identified SNRs are in general not detected. This lends more support to the hypothesis that searches conducted for SNRs at each wavelength – X-ray, optical and radio – all possess inherent biases. We also find additional evidence that the density of the ambient ISM surrounding an SNR plays a critical role in dictating the SNR's spectral characteristics.

3) A search for non-thermal radio sources at 6 cm and 20 cm (with a minimum detection level of 3σ) that are close to or within HII regions has yielded five candidate radio SNRs. Of these five sources, one (NGC 7793-R3) possesses an X-ray counterpart at the 3σ level, namely P10, from the listing of X-ray sources in this galaxy that was prepared by RP99. Another candidate radio SNR, NGC 7793-R4, may also contribute X-ray flux to P10.

4) A search for candidate X-ray SNRs has not revealed any new sources in addition to the SNRs already found through radio and optical surveys. The search for SNRs at this wavelength is complicated by the presence of considerable diffuse X-ray emission throughout the entire disk of this galaxy.

5) The multi-wavelength campaign has added five new candidate SNRs to the 28 previously identified through optical methods. While the number of new detected SNRs is noticeably lower than the number of new SNRs found in our study of NGC 300 as presented in Paper I, we feel that this result is linked to the larger distance to NGC 7793 than NGC 300. Because the X-ray and radio observations of NGC 7793 did not have improved sensitivities to compensate for the increased distance to this galaxy compared to NGC 300, both surveys can only sample more luminous portions of the X-ray and radio SNR population in NGC 7793 compared to NGC 300.

This paper is derived in large part from the Ph.D dissertation of T. G. P., conducted at the University of New Mexico. We thank the referee, Schuyler Van Dyk, for many useful comments and suggestions which have greatly improved this work. T. G. P. acknowledges fruitful discussions with Glenn E. Allen and Miroslav Filipović. This research has made use of NASA's Astrophysics Data System Abstract Service and the NASA/IPAC Extragalactic Database (NED) which is operated by the Jet Propulsion Laboratory, California Institute of Technology, under contract with the National Aeronautics and Space Administration. The *ROSAT* project is supported by the German Bundesministerium für Bildung und Forschung (BMBF) and the Max-Planck-Gesellschaft (MPG). T. G. P. gratefully acknowledges support from both the *Chandra* X-ray Center High Energy Transmission Grating (HETG) group through grant NAS8-38249 and the NRAO.

REFERENCES

Allen, G.E., et al. 1997, ApJ, 487, L97

Bartunov, O.S., Tsvetkov, D. Yu. & Filimonova, I.V. 1994, PASP, 106, 1276

Blair, W.P. & Long, K.S. 1997, ApJS, 108, 261 (BL97)

Carignan, C. 1985, ApJS, 58, 107

Carignan, C. & Puche, D. 1990, AJ, 100, 394

D'Odorico, S., Dopita, M.A. & Benvenuti, P. 1980, A&AS, 40, 67

Fabbiano, G., Kim, D.-W. & Trinchieri, G. 1992, ApJS, 80, 531

Ferguson, A.M.N., Wyse, R.F.G., Gallagher, J.S., III & Hunter, D.A. 1996, AJ, 111, 2265

Freedman, W.L., Madore, B.F., Hawley, S.L., Horowitz, I.K., Mould, J. & Sallmen, S. 1992, ApJ, 396, 80

Gordon, S.M., Kirshner, R.P., Long, K.S., Blair, W.P., Duric, N. & Smith, R.C. 1998, ApJS, 117, 89

Gordon, S.M., Duric, N., Kirshner, R.P., Goss, W.M. & Viallefond, F. 1999, ApJS, 120, 247

Greenawalt, B.E., Walterbos, R.A.M., Thilker, D. & Hoopes, C.G. 1998, ApJ, 506, 135

Haberl, F. & Pietsch, W. 2001, A&A, 373, 438

Harnett, J.I. 1986, PASAu, 6, 325

Hasinger, G., Turner, T.J., George, I.M. & Boese, G. 1992, OGIP Calibration Memo CAL/ROS/92-001

Hodge, P.W. 1969, ApJS, 157, 73

Hoopes, C.G., Walterbos, R.A.M. & Greenawalt, B.E. 1996, AJ, 112, 1429

Hwang, U., Petre, R. & Hughes, J. P. 2000, ApJ, 532, 970

Lacey, C.K., Duric, N. & Goss, W.M. 1997, ApJS, 108, 417

Lacey, C.K. & Duric, N. 2001, ApJ, 560, 719

Lacey, C.K., Lazio, T.J.W., Kassim, N.E., Duric, N., Briggs, D.S. & Dyer, K. K. 2001, ApJ, 559, 954

Long, K.S., Charles, P.A., Blair, W.P. & Gordon, S.M. 1996, ApJ, 466, 750

Matonick, D.M. & Fesen, R.A. 1997, ApJS, 112, 49

Matonick, D.M., Fesen, R.A., Blair, W.P. & Long, K.S. 1997, ApJS, 113, 333

Mitchell, K.J. & Condon, J.J. 1985, AJ, 90, 1957

Pannuti, T.G., Duric, N., Lacey, C.K., Goss, W.M., Hoopes, C.G., Walterbos, R.A.M. & Magnor, M. 2000, ApJ, 544, 780 (Paper I)

Puche, D. & Carignan, C. 1988, AJ, 95, 1025

Read, A.M., Ponman, T.J. & Strickland, D.K. 1997, MNRAS, 286, 626

Read, A.M. & Pietsch, W. 1999, A&A, 341, 8 (RP99)

Read, A.M. & Pietsch, W. 2001, A&A, 373, 473

Schulz, N.S. 1999, ApJ, 511, 304

Trümper, J. 1992, QJRAS, 33, 165

Tully, R. 1988, *Nearby Galaxies Catalog* (Cambridge: Cambridge University Press)

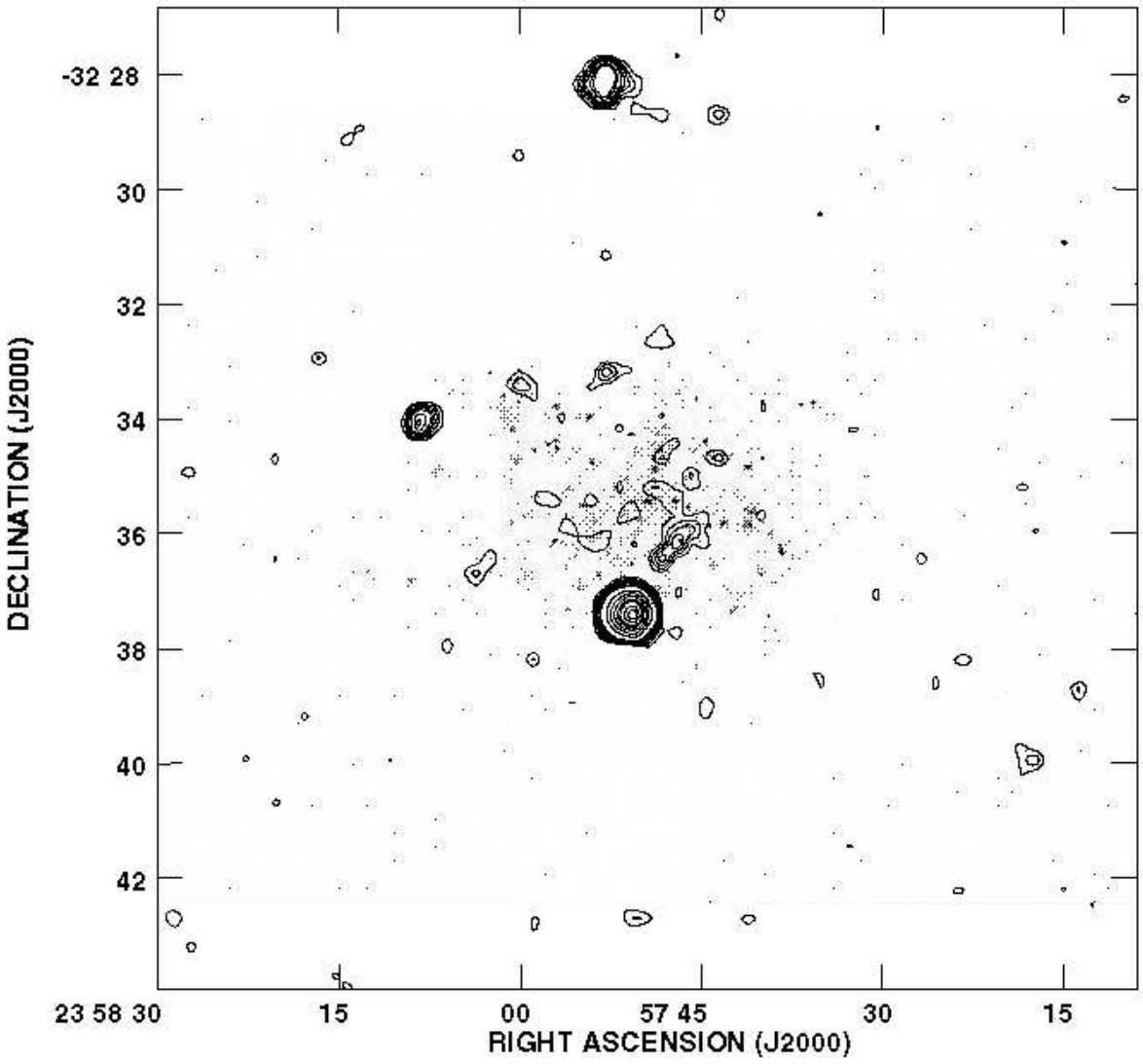

Fig. 1.— X-ray (contours) and Hα (gray-scale) image of NGC 7793. The Hα image was prepared using observations made with the CTIO, while the X-ray image was prepared using observations made with the ROSAT PSPC instrument over the total energy range of 0.1-2.4 keV with a combined integration time of 23839 sec. The noise level in the X-ray image is 9.4×10^{-4} counts per square arcminute, and the contours are set at the 3σ, 4.5σ, 6σ, 7.5σ, 9σ, 12σ, 14σ, 30σ, 45σ, 60σ, 75σ, 85σ, 105σ and 120σ level.

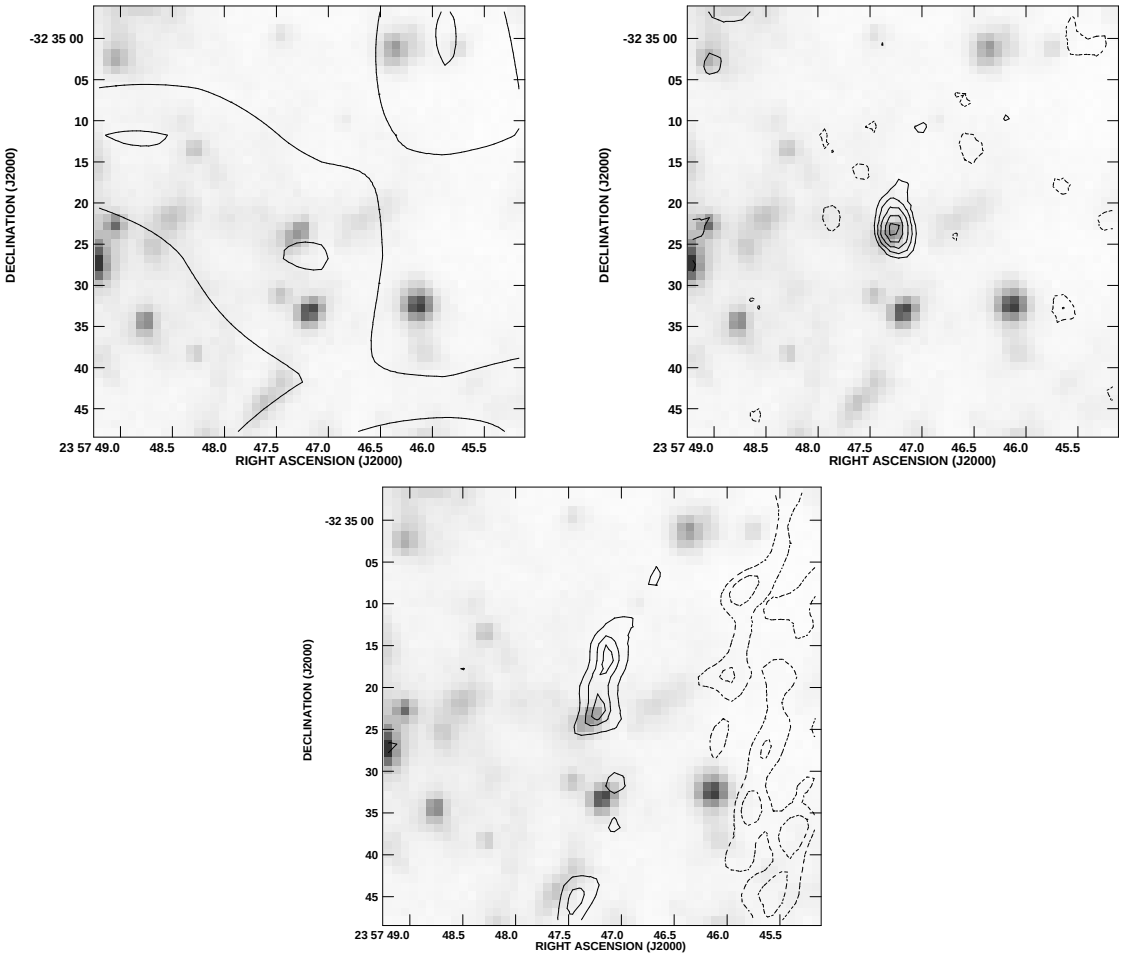

Fig. 2.— Multi-wavelength images of the environment surrounding the optically-identified SNR N7793-S11. In each image, the Hα emission is depicted in gray scale. X-ray emission (as observed by the PSPC instrument) is depicted in Fig. 2a (the upper left figure), using the same contour levels as in Figure 1. Emission at the 6 and 20 cm is depicted in contours in Fig. 2b and 2c (the upper right and lower figures), respectively. In Fig. 2b, the contours are placed at -3, -2, 3, 4, 5, 6 and 6.75 times the rms noise level at 6 cm (32 μJy), and in Fig. 2c, the contours are placed at -3, -2, 3, 4 and 4.5 times the rms noise level at 20 cm (60 μJy). The approximate beam sizes are $\approx 6''$ in both the 6 and 20 cm images. See § 3.

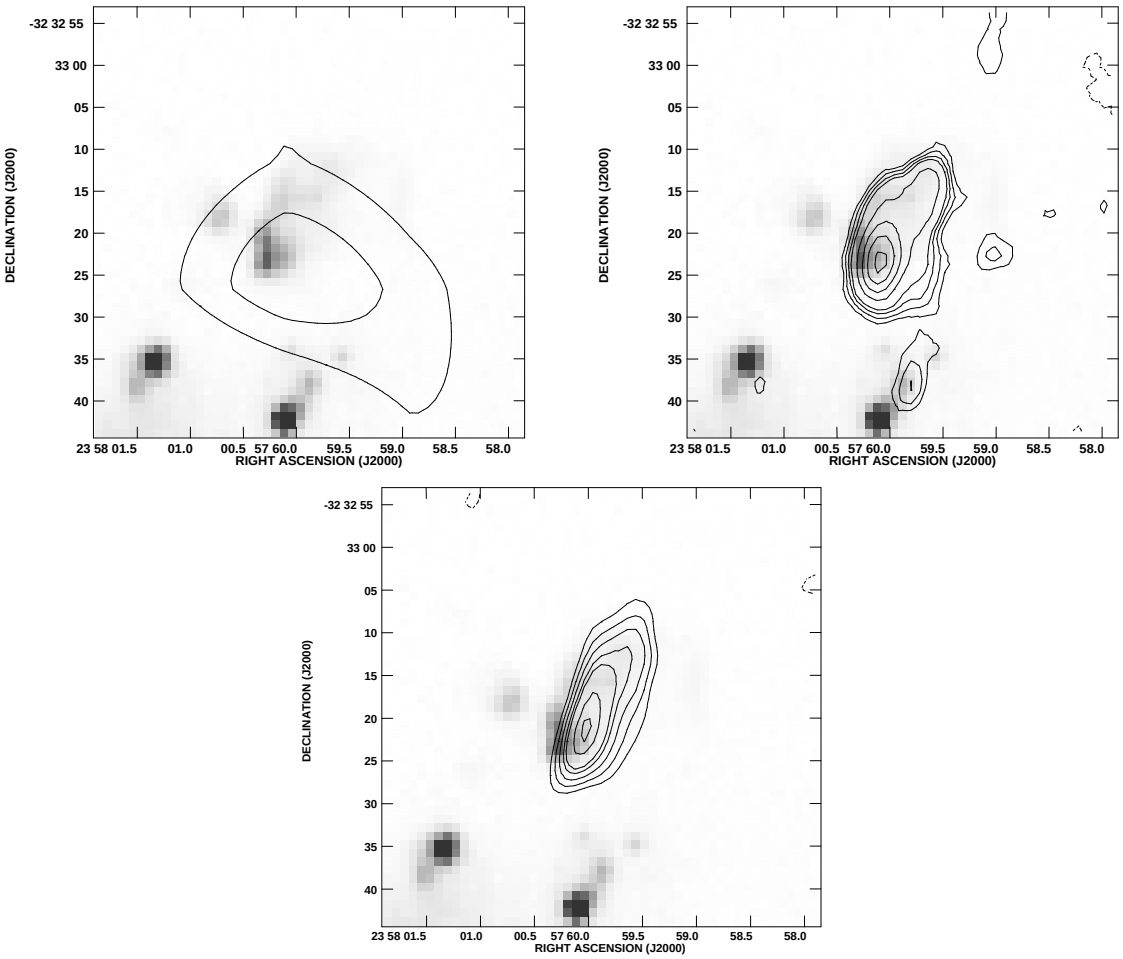

Fig. 3.— Same as Fig. 2, but for the optically identified SNR N7793-S26. Notice the filamentary structure apparent in both Hα emission and radio emission, as well as the coincidence with the X-ray source P8 as seen in Fig. 3a. In Fig. 3b, the contours are placed at -3, -2, 3, 4, 5, 6, 9, 12, 15 and 18 times the rms noise level at 6 cm, and in Fig. 3c, the contours are placed at -3, -2, 9, 12, 15, 18, 20, 25 and 28 times the rms noise level at 20 cm. See § 3.

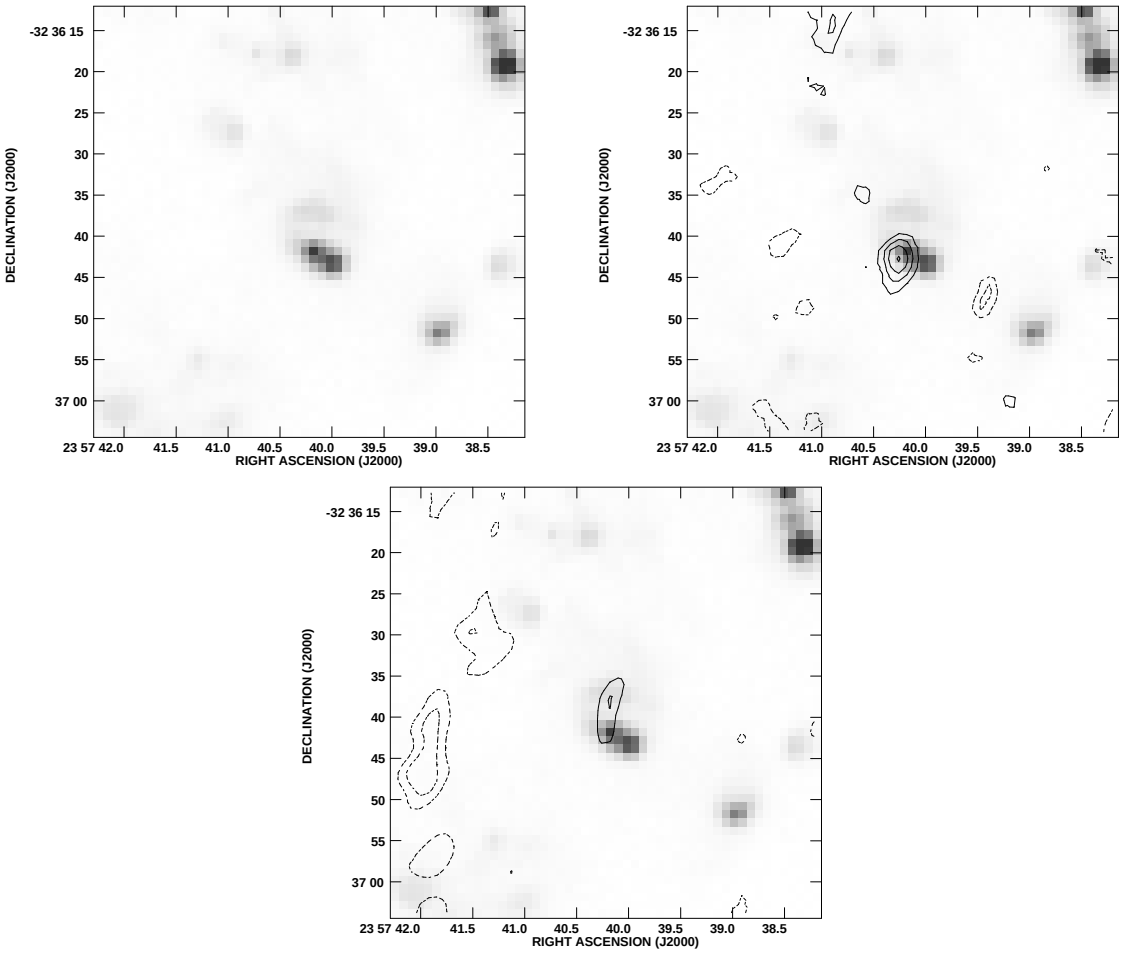

Fig. 4.— Same as Fig. 2, but for the candidate radio SNR NGC 7793-R1 in the HII region Hodge 31. In Fig. 4b, the contours are placed at -3, -2, 3, 4, 5 and 6 times the rms noise level at 6 cm, and in Fig. 4c, the contours are placed at -3, -2, 3 and 3.5 times the rms noise level at 20 cm. See § 4.

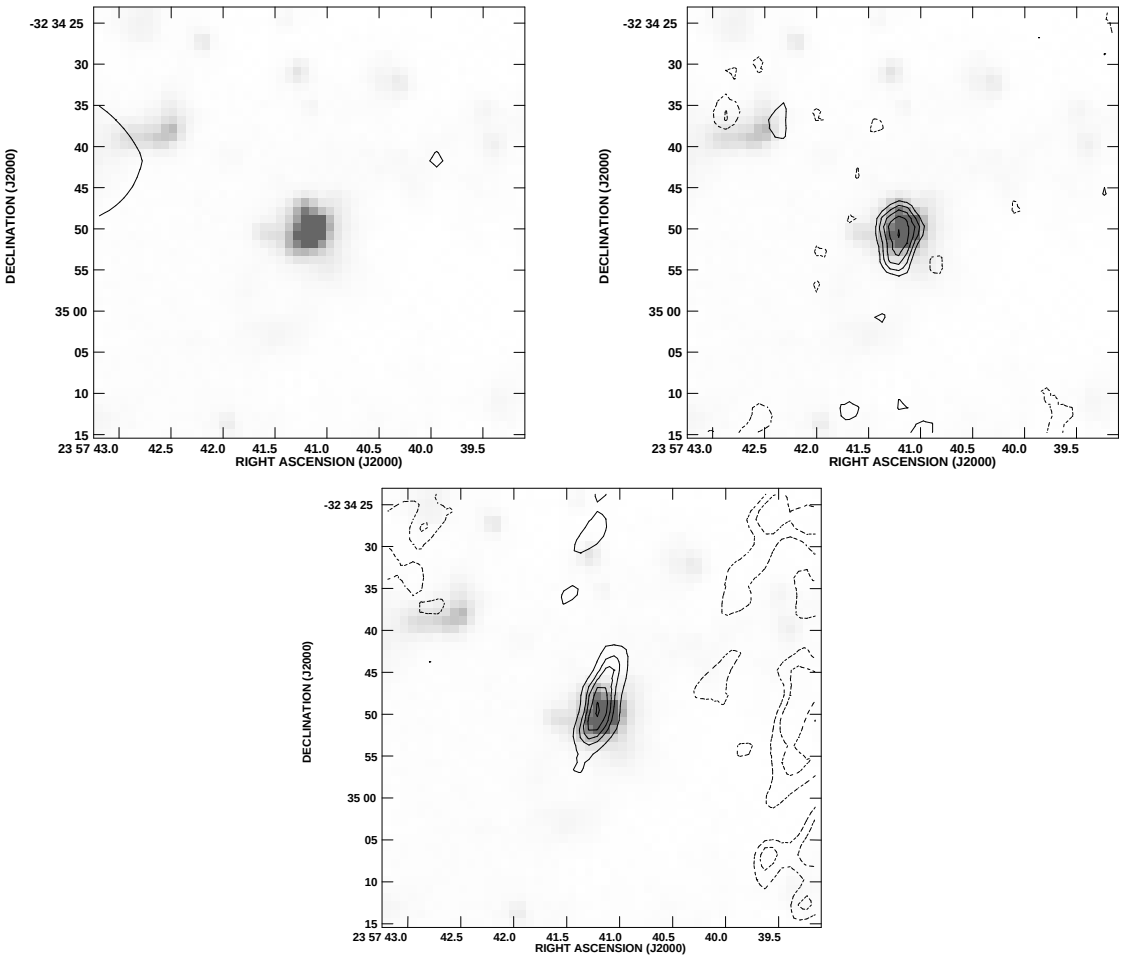

Fig. 5.— Same as Fig. 2, but for the candidate radio SNR NGC 7793-R2 in the HII region Hodge 27. In Fig. 5b, the contours are placed at -3, -2, 3, 4, 5, 6 and 7 times the rms noise level at 6 cm, and in Fig. 5c, the contours are placed at -3, -2, 3, 4, 4.5, 5 and 5.5 times the rms noise level at 20 cm. See § 4.

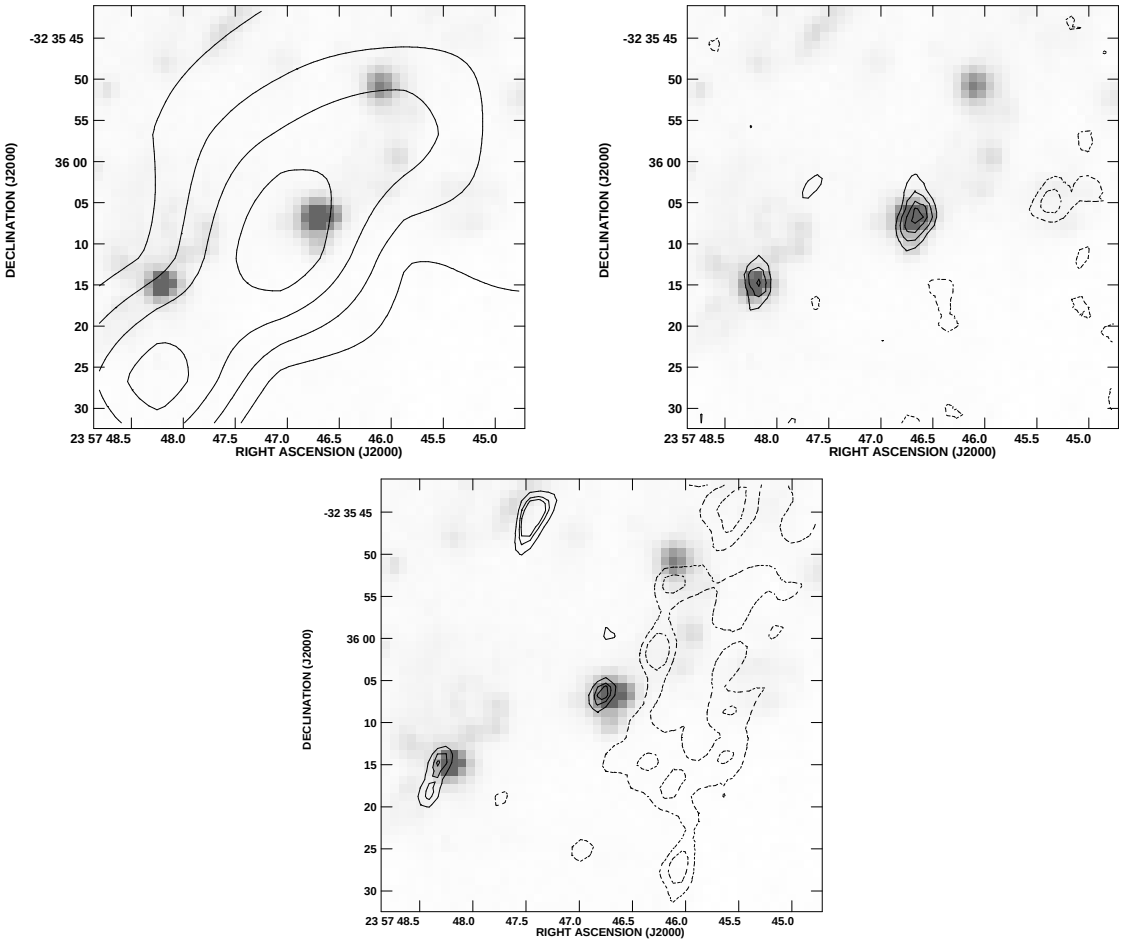

Fig. 6.— Same as Fig. 2, but for the candidate radio SNR NGC 7793-R3 in the HII region Hodge 23. In Fig. 6a, notice the proximity to the X-ray source P10. In Fig. 6b, the contours are placed at -3, -2, 3, 4, 5 and 5.75 times the rms noise level at 6 cm, and in Fig. 6c, the contours are placed at -3, -2, 3, 3.5 and 3.75 times the rms noise level at 20 cm. See § 4.

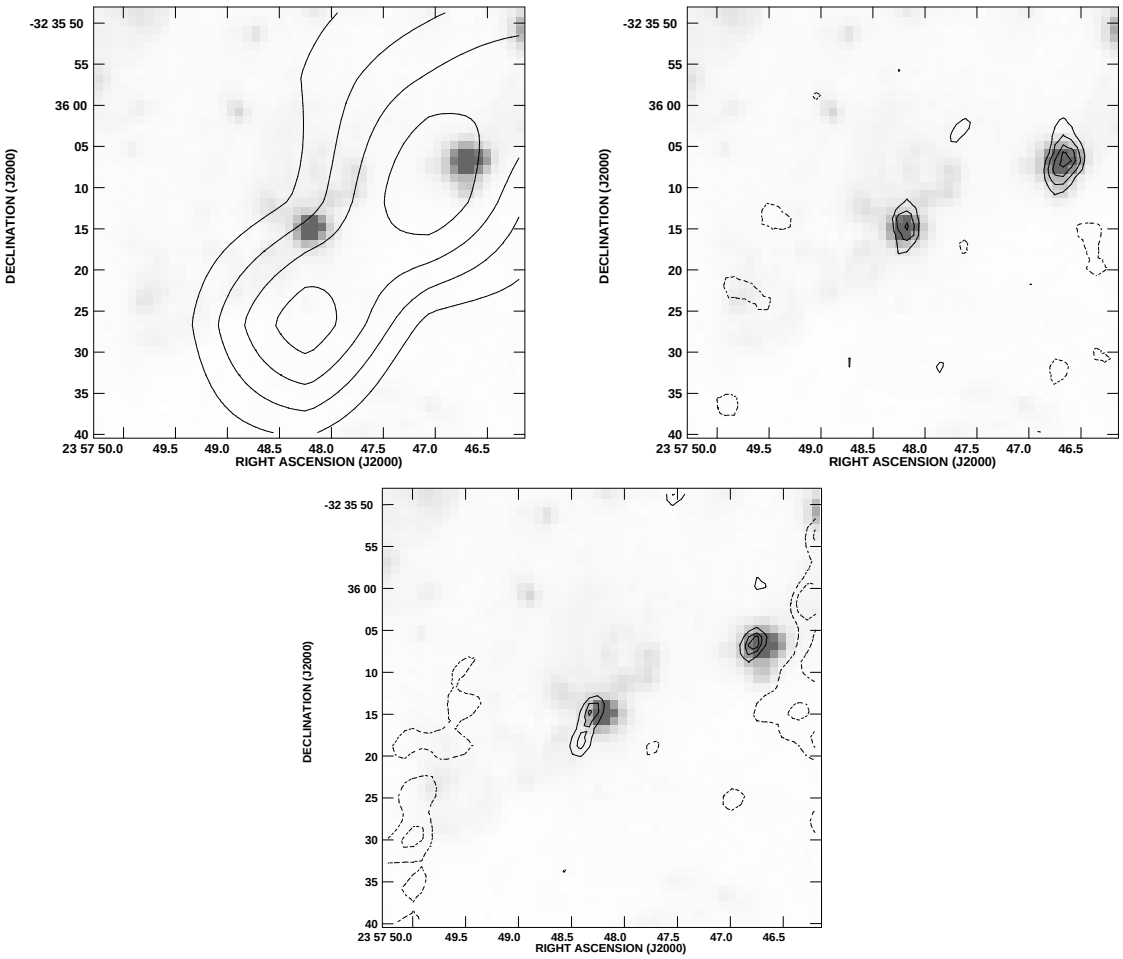

Fig. 7.— Same as Fig. 2, but for the candidate radio SNR NGC 7793-R4 in the HII region Hodge 21. In Fig. 7b, the contours are placed at -3, -2, 3, 4, 5 and 5.75 times the rms noise level at 6 cm, and in Fig. 7c, the contours are placed at -3, -2, 3, 3.5 and 3.75 times the rms noise level at 20 cm. See § 4.

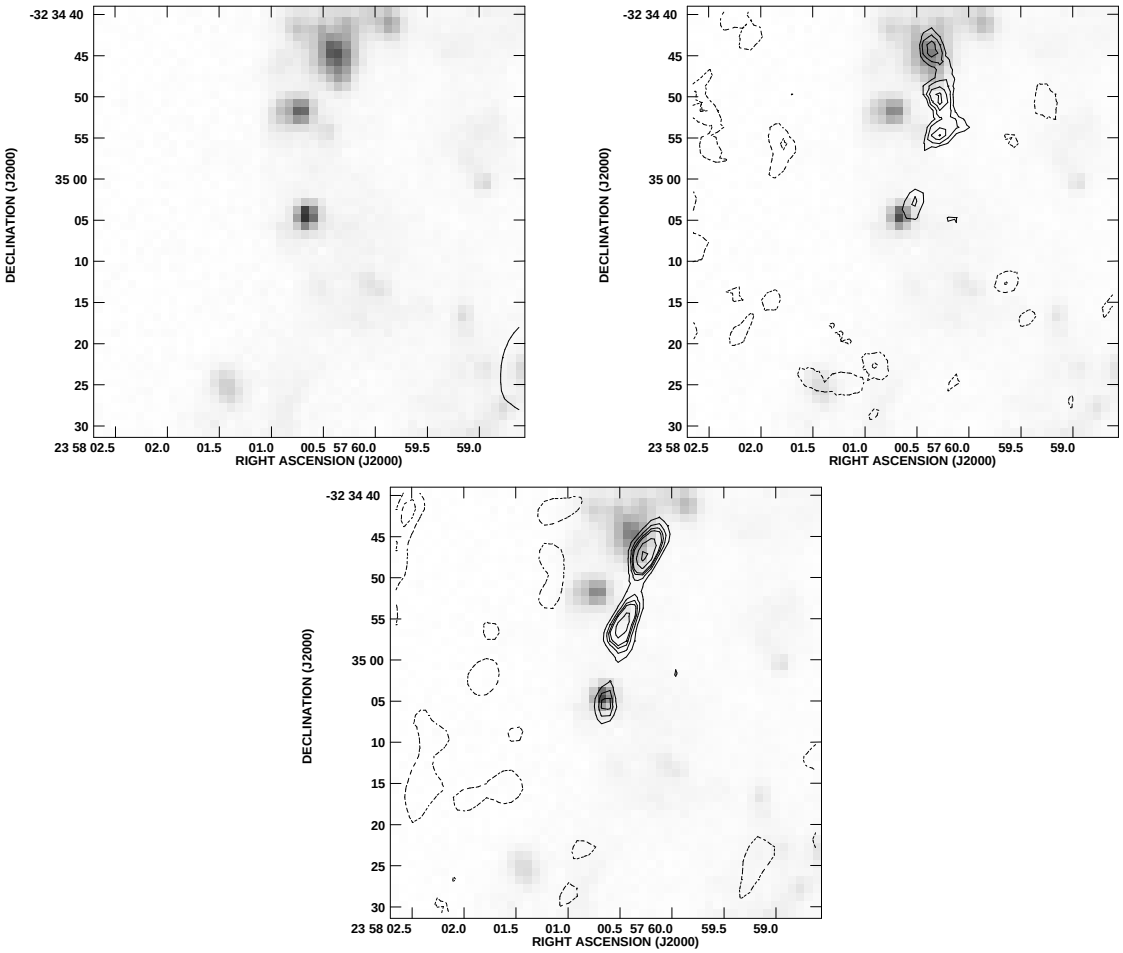

Fig. 8.— Same as Fig. 2, but for the candidate radio SNR NGC 7793-R5 in an uncataloged HII region. In Fig. 8b, the contours are placed at -3, -2, 3, 3.5, 4 and 4.5 times the rms noise level at 6 cm, and in Fig. 8c, the contours are placed at -3, -2, 3, 3.8, 4, 4.5 and 5 times the rms noise level at 20 cm. See § 4.

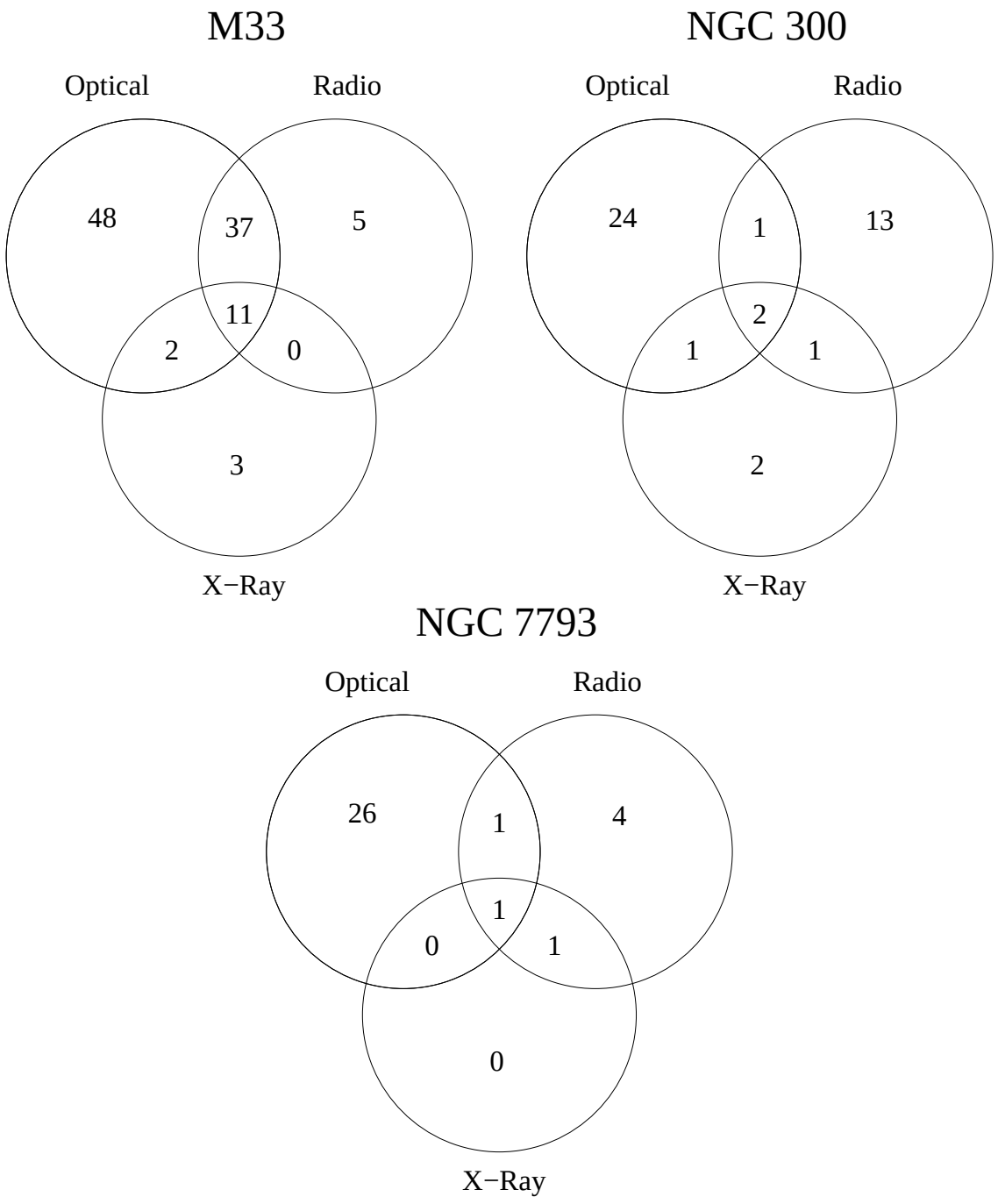

Fig. 9.— Venn Diagrams depicting the intersection of selected sets of SNRs (X-ray, optical and radio) for the galaxies M33, NGC 300 and NGC 7793. The galaxies have been arranged in order of increasing distance. Notice how limited the intersection between the three sets becomes with increasing distance to the galaxy.

Table 1. General Properties of NGC 7793

Property	NGC 7793
R.A. (J2000.0)	23h 57m 49.2s[a]
Dec (J2000.0)	-32° 35′ 24″[a]
Galactic Latitude	-77.17[a]
Galactic Longitude	4.52[a]
Observed Diameter D_{25} (arcmin)	9.2[b]
Axial Ratio d/D	0.70[b]
N_H Column Density (cm^{-2})	1.14×10^{20}[c]
Hubble Type	SA(s)d[a]
Distance (Mpc)	3.38[d]
Inclination i ($^\circ$)	50[b]

[a]NED Database.

[b]Tully (1988).

[c]RP99.

[d]Puche & Carignan (1988).

Table 2. Parameters of the NGC 7793 Observations with the VLA

Configuration	Frequency (GHz)	Field of View (arcmin)	Sensitivity (μJy)	Linear Resolution (pc)	Synthesized Beam (arcsec^2)	Position Angle (degrees)
CnB	4.86	9	32	97	7.8×4.2	-3.63
BnA	1.47	27	60	97	9.4×4.1	-10.25

Table 3. Radio-Selected SNR Candidates in NGC 7793

Source Name	RA (J2000.0)	Dec (J2000.0)	S_6 (mJy)	δS_6 (mJy)	S_{20} (mJy)	δS_{20} (mJy)	α[a]	$\delta\alpha$
N7793-S11	23 57 47.3	−32 35 23	0.21	0.10	0.45	0.15	+0.6	0.5
N7793-S26[b]	23 58 00.0	−32 33 19	1.24	0.19	3.75	0.30	+0.9	0.2
NGC 7793-R1	23 57 40.2	−32 37 38	<[c]	0.10	0.22	0.07	>0.7	–
NGC 7793-R2	23 57 41.2	−32 34 50	0.24	0.08	0.39	0.13	+0.4	0.4
NGC 7793-R3	23 57 46.8	−32 36 07	0.22[d]	0.04	0.26	0.07	+0.2	0.3
NGC 7793-R4	23 57 48.4	−32 36 15	0.16[d]	0.04	0.22	0.07	+0.3	0.3
NGC 7793-R5	23 58 00.7	−32 35 06	0.12	0.04	0.25	0.07	+0.6	0.4

Note. — Units of right ascension are hours, minutes and seconds, and units of declination are degrees, arcminutes and arcseconds.

[a]$S_\nu \propto \nu^{-\alpha}$.

[b]Here we refer to the combination of the two sources denoted as "N7793-S26" and "N7793-S26ext" as one source.

[c]Not detected at the 3σ level at this wavelength.

[d]Diffuse radio emission from the adjacent HII region makes isolating the radio emission associated with the SNR difficult at this wavelength.

Table 4. Properties of X-ray Sources in NGC 7793

Source Number	RA (J2000.0)	Dec (J2000.0)	Net Counts	Flux (10^{-14} ergs cm^{-2} sec^{-1})	Hardness Ratio	Probability of Variability	Optical/Radio Counterparts
P6	23 57 48.5	−32 32 30	41.3±9.6	2.3±0.5	+0.1±0.2	41%	–
P7	23 57 52.6	−32 33 11	54.7±10.1	3.0±0.6	+0.2±0.2	37%	–
P8	23 57 59.8	−32 33 24	69.5±12.0	3.9±0.7	+0.1±0.2	13%	N7793-S26
P9	23 58 08.6	−32 34 03	110.1±12.5	6.2±0.7	>0.5	100%	–
P10	23 57 47.1	−32 36 05	173.4±18.1	9.7±1.0	+0.1±0.1	7%	H23, R3 (H21?, R4?)
P11	23 58 03.1	−32 36 34	41.2±9.3	2.3±0.5	>0.2	37%	–
P13	23 57 51.2	−32 37 23	976.0±32.0	54.9±1.8	+0.9±0.0	100%	–

Table 5. Corrected Positions of Optically-Identified SNRs in NGC 7793

SNR	RA (J2000.0)	Dec (J2000.0)	SNR	RA (J2000.0)	Dec (J2000.0)
N7793-S1	23 57 38.59	−32 34 37.4	N7793-S16	23 57 54.57	−32 35 12.1
N7793-S2	23 57 38.66	−32 33 19.0	N7793-S17	23 57 55.40	−32 33 52.9
N7793-S3	23 57 39.11	−32 35 38.5	N7793-S18	23 57 55.40	−32 34 33.4
N7793-S4	23 57 40.61	−32 35 51.7	N7793-S19	23 57 55.86	−32 37 21.5
N7793-S5	23 57 41.02	−32 37 02.6	N7793-S20	23 57 56.07	−32 37 17.5
N7793-S6	23 57 43.78	−32 35 27.1	N7793-S21	23 57 56.62	−32 36 09.8
N7793-S7	23 57 44.05	−32 36 40.6	N7793-S22	23 57 58.50	−32 35 23.1
N7793-S8	23 57 44.96	−32 37 41.3	N7793-S23	23 57 59.03	−32 36 46.7
N7793-S9	23 57 44.99	−32 37 35.1	N7793-S24	23 57 59.34	−32 36 06.7
N7793-S10	23 57 45.76	−32 35 00.7	N7793-S25	23 57 59.83	−32 36 19.0
N7793-S11	23 57 47.26	−32 35 23.1	N7793-S26	23 58 00.27	−32 33 22.1
N7793-S12	23 57 48.30	−32 36 56.0	N7793-S26ext	23 57 59.79	−32 33 16.0
N7793-S13	23 57 51.26	−32 36 32.2	N7793-S27	23 58 06.75	−32 35 12.5
N7793-S14	23 57 52.58	−32 33 52.5	N7793-S28	23 58 06.75	−32 35 36.7
N7793-S15	23 57 54.36	−32 34 02.6			

Table 6. Cross-References of All New Candidate Radio SNRs in NGC 7793

Candidate Radio SNR[a]	RA (J2000.0)	Dec (J2000.0)	Optical Counterpart?	X-ray Counterpart?
NGC 7793-R1	23 57 40.2	−32 37 38	H31	–
NGC 7793-R2	23 57 41.2	−32 34 50	H27	–
NGC 7793-R3	23 57 46.8	−32 36 07	H23	P10
NGC 7793-R4	23 57 48.4	−32 36 15	H21	(P10?)
NGC 7793-R5	23 58 00.4	−32 35 06	Uncataloged HII Region	–

[a]In this table, the radio counterparts are the radio sources presented in Table 3, the optical counterparts are the HII regions cataloged by Hodge (1969), and the X-ray counterparts are the X-ray sources listed in Table 4.

Table 7. Sensitivities of SNR Surveys of M33, NGC 300 and NGC 7793

Galaxy	X-ray (counts sec^{-1} $arcmin^{-2}$)	Reference	Hα (ergs cm^{-2} sec^{-1} $arcsec^{-2}$)	Reference	20 cm (μJy per beam)	Reference
M33	9×10^{-4}	(1)	$\sim 6 \times 10^{-17}$	(2)	50	(3)
NGC 300	1.2×10^{-3}	(4)	$\sim 1 \times 10^{-16}$	(5)	60	(6)
NGC 7793	1.7×10^{-3}	(7)	$\sim 1 \times 10^{-16}$	(5)	60	(8)

Note. — The references used in this table are as follows: (1) Haberl & Pietsch (2001), (2) Gordon et al. (1998), (3) Gordon et al. (1999), (4) Read & Pietsch (2001), (5) BL97, (6) Paper I, (7) RP99 and (8) This work.